Journal of Fluids Engineering

Technical Briefs

Unsteady Flow of a Power-Law Dusty Fluid With Suction

Ali J. Chamkha[1]

Equations governing flow of a particulate suspension exhibiting finite volume fraction in non-Newtonian power-law fluids are developed and applied to the problem of unsteady flow past an infinite porous flat plate with suction. Numerical results for small volume fraction for the displacement thicknesses for both phases and the skin-friction coefficient for the fluid phase are obtained using an implicit finite difference scheme and presented graphically to elucidate interesting features of the solutions.

Introduction

Much of the two-phase (particle-fluid) flow research treats the fluid phase as Newtonian in nature. This is because this type of fluids exhibits a linear relationship between the shear stress and the shear rate. However, many fluids of practical applications are non-Newtonian. Since particulate suspensions in non-Newtonian power-law fluids are encountered in wide variety of the process industry, it is of interest to understand their characteristics.

The problem of steady single-phase flow of a Newtonian fluid past a flat plate with uniform suction was solved exactly and reported some time ago by Schlichting (1955). Kapur (1963) obtained steady-state solutions for flow of pseudo-plastic and dilatant power-law fluids past a porous flat plate. Chamkha and Peddieson (1989) reported solutions for unsteady flow of a particulate suspension past an infinite flat plate with uniform fluid-phase suction. In their work, Chamkha and Peddieson (1989) considered only Newtonian fluids.

The aim of this paper is to extend the work of Chamkha and Peddieson (1989) to particulate suspensions in non-Newtonian power-law fluids. Both phases are modeled as interacting continua and the interphase forces between the two phases is modeled by Stokes linear drag theory. The continuum modeling approach of two-phase suspensions has been the subject of numerous papers (see, for instance, Hinze, 1963). The advantages of this approach lie in the simplification of the general transport equation of kinetic theory of flow by replacing phase change coordinates with space coordinates. This is done through the introduction of phenomenological relations and transport properties to account for viscous stresses, heat fluxes, and mass generations. In addition, this approach is applicable to fluids (such as liquids) whose microscopic details are unknown (see, Soo, 1990).

Governing Equations

Let the plate be situated along the x-axis at $y=0$ with the y-axis being normal to it. Let the flow be a uniform stream in the x-direction parallel to the plate. Far above the plate, assume that both phases are in equilibrium and moving with the free stream velocity V_∞. Further assume that fluid-phase suction with velocity V_s is imposed at the plate surface. In the development of the governing equations, it is also assumed that both phases are incompressible, the fluid-phase pressure gradient is negligible, and the volume fraction of suspended particles is finite and uniform.

To formulate the governing equations for the problem described above, the balance laws of mass and linear momentum for both the fluid and particulate phases along with constitutive equations for the stress tensors and the interphase force are used.

The balance laws of mass (for the fluid and particulate phases, respectively) can be written as

$$\partial_t \phi - \nabla \cdot ((1-\phi)\mathbf{V}) = 0, \; \partial_t \phi + \nabla \cdot (\phi \mathbf{V}_p) = 0 \quad (1)$$

where ϕ is the particulate volume fraction, ∇ is the gradient operator, $\mathbf{V}$ is the fluid-phase velocity vector, and $\mathbf{V}_p$ is the particulate-phase velocity vector.

The balance laws of linear momentum (for the fluid and particulate phases, respectively) can be written as

$$\rho(1-\phi)(\partial_t \mathbf{V} + \mathbf{V} \cdot \nabla \mathbf{V}) = \nabla \cdot \underline{\underline{\sigma}} - \mathbf{f}, \; \rho_p \phi (\partial_t \mathbf{V}_p + \mathbf{V}_p \cdot \nabla \mathbf{V}_p) = \nabla \cdot \underline{\underline{\sigma}}_p + \mathbf{f} \quad (2)$$

where ρ is the fluid-phase density, $\underline{\underline{\sigma}}$ is the fluid-phase stress tensor, $\mathbf{f}$ is the interphase force per unit volume acting on the particle phase, ρ_p is the particle-phase density, and $\underline{\underline{\sigma}}_p$ is the particle-phase stress tensor.

Equations (1) and (2) are supplemented with the following constitutive equations

$$\underline{\underline{\sigma}} = (1-\phi)(-P\underline{\underline{I}} + 2\mu(\mathrm{II}, \phi)\underline{\underline{D}})$$
$$\underline{\underline{\sigma}}_p = \phi(-P_p\underline{\underline{I}} + 2\mu_p(\mathrm{II}_p, \phi)\underline{\underline{D}}_p)$$
$$\underline{\underline{D}} = \frac{1}{2}(\nabla \mathbf{V} + \nabla \mathbf{V}^T), \; \underline{\underline{D}}_p = \frac{1}{2}(\nabla \mathbf{V}_p + \nabla \mathbf{V}_p^T)$$
$$\mathrm{II} = \underline{\underline{D}}:\underline{\underline{D}}, \; \mathrm{II}_p = \underline{\underline{D}}_p:\underline{\underline{D}}_p, \; \mathbf{f} = N\rho_p\phi(\mathbf{V} - \mathbf{V}_p) \quad (3)$$

where P is the fluid-phase pressure, P_p is the particle-phase pressure, $\underline{\underline{I}}$ is the unit tensor, μ is the fluid-phase dynamic viscosity, μ_p is the particle-phase dynamic viscosity, $\underline{\underline{D}}$ is the fluid-phase rate of strain tensor, $\underline{\underline{D}}_p$ is the particle-phase rate of strain tensor, II is the second invariant of $\underline{\underline{D}}$, II_p is the second invariant of $\underline{\underline{D}}_p$, N is a momentum transfer coefficient,

[1]Staff Research Engineer, Fleetguard, Inc., Cookeville, TN 38502. Mem. ASME.

Contributed by the Fluids Engineering Division of THE AMERICAN SOCIETY OF MECHANICAL ENGINEERS. Manuscript received by the Fluids Engineering Division June 4, 1992; revised manuscript received December 2, 1992. Associate Technical Editor: M. W. Reeks.

and a superposed T denotes the transpose of a second-order tensor. In the present work ρ, ρ_p, and N will all be treated as constants.

For small particulate volume fraction $(\phi << 1)$ $\mu = \mu(\mathrm{II}) = (2\mathrm{II})^{(n-1)/2}$ (n is a behavior coefficient), $\mu_p = 0$ (negligible particle-particle interaction), and $P_p = 0$ (see, for instance, Marble, 1970). The behavior coefficient n determines whether the fluid is Newtonian ($n=1$) or non-Newtonian ($n \neq 1$).

It is convenient to nondimensionalize the governing differential equations given previously for small volume fraction by using

$$t = \nu\tau/V_\infty^2,\ y = \nu\eta/\mathbf{V}_\infty,\ \mathbf{V} = \mathbf{e}_x V_\infty F(\tau,\eta) - \mathbf{e}_y \mathbf{V}_s$$

$$\mathbf{V}_p = \mathbf{e}_x \mathbf{V}_\infty F_p(\tau,\eta) - \mathbf{e}_y \mathbf{V}_s,\ \nu = V_\infty^{2(1-1/n)}(c/\rho)^{1/n} \quad (4)$$

where c is a constant and $\mathbf{e}_x$ and $\mathbf{e}_y$ are unit vectors in the x and y directions, respectively.

Substituting Eqs. (4) into Eqs. (1) through (3) and rearranging yield

$$\partial_\tau F - \partial_\eta((\partial_\eta F)^n) - r_v\, \partial_\eta F + \kappa\alpha(F - F_p) = 0 \quad (5)$$

$$\partial_\tau F_p - r_v \partial_\eta F_p - \alpha(F - F_p) = 0 \quad (6)$$

where $r_v = V_s/V_\infty$, $\kappa = \rho_p\phi/\rho$, $\alpha = N\nu/V_\infty^2$ are the suction parameter, the particle loading, and the inverse Stokes number, respectively. Equations (5) and (6) represent the non-Newtonian power-law version of the dusty-gas model discussed by Marble (1970). It should be mentioned that ρ_p/ρ is very large and ϕ is very small such that $\rho_p\phi/\rho$ is finite. Therefore, κ could be equal to 1, 10, or even 100 and still apply to low particulate concentrations.

The initial and boundary conditions used to solve Eqs. (5) and (6) are

$$F(0,\eta) = 1.0,\ F_p(0,\eta) = 1.0,\ F(\tau,0) = 0$$

$$\lim_{\eta\to\infty} F(\tau,\eta) = 1.0,\ \lim_{\eta\to\infty} F_p(\tau,\eta) = 1.0 \quad (7)$$

The fluid-phase displacement thickness, the particle-phase displacement thickness, and the fluid-phase skin-friction coefficient are defined as follows:

$$\delta = \int_0^\infty (1-F)d\eta,\ \delta_p = \int_0^\infty (1-F_p)\,d\eta,\ C_f = (\partial_\eta F(\tau,0))^n \quad (8)$$

Results

Closed-form solutions of Eqs. (5) and (6) are possible for dilute suspensions ($\kappa = 0$) and steady-state conditions. When $\kappa = 0$, the fluid-phase motion is independent of the presence of particles and Eq. (5) can be solved for F subject to Eqs. (7) to yield

$$F = 1 - (1 - (n-1)/n r_v^{1/n}\eta)^{n/n-1)} \quad (9)$$

The corresponding form of F_p obtained by solving Eq. (6) and using Eq. (9) is

$$F_p = 1 - \alpha/r_v \exp(\alpha/r_v\eta)\int_\eta^\infty \exp(-\alpha/r_v\eta)$$

$$\times (1-(n-1))/n r_v^{1/n}\eta)^{\ n/(n-1)} d\eta \quad (10)$$

Equation (10) can be carried out for specific values of n. In general, it can be solved numerically for any value of n. For a dilatant fluid ($n > 1$) it can be shown from Eq. (9) that the fluid-phase tangential velocity F approaches the free stream value after a finite height above the plate. This is given by

$$\eta_0 = n/((n-1)\ r_v^{1/n}) \quad (11)$$

Thus,

$$F = 1 - (1-\eta/\eta_0)^{n(n-1)}\ ;\ \eta \le \eta_0$$

$$F = 1 \qquad ;\ \eta > \eta_0 \quad (12)$$

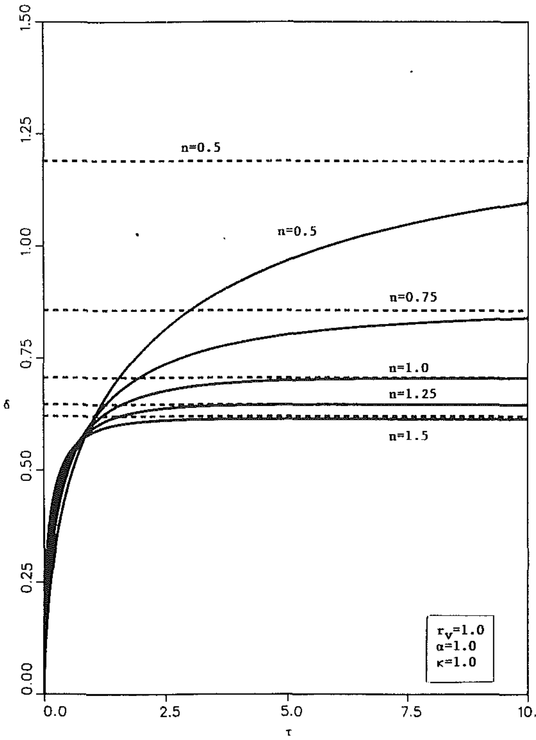

Fig. 1 Fluid-phase displacement thickness profiles

$$F_p = 1 - \alpha/r_v \exp(\alpha/r_v\eta)\int_\eta^{\eta_0} \exp(-\alpha/r_v\eta)(1-\eta/\eta_0)^{n/(n-1)} d\eta$$

$$;\eta \le \eta_0$$

$$F_p = 1 \qquad ;\eta > \eta_0 \quad (13)$$

The integral appearing in Eq. (13) can be carried out further for some values of $n > 1$ such that $k = n/(n-1)$ is an integer. This can be shown to give

$$F_p = 1 - \sum_{r=1}^{\infty} ((-1)^r k!(1-\eta/\eta_0)^{k-r})/(k-r)!(\alpha/r_v\eta_0)^r);\eta \le \eta_0 \quad (14)$$

The initial-value problem consisting of Eqs. (5) through (7) is solved numerically using an extension of the implicit finite difference method described by Blottner (1970) to two-phase flow. The main components of the numerical method is the application of variables step sizes in the η and τ directions, and the iteration procedure. Since the largest changes in the dependent variables are expected to occur in the region close to the plate's surface, a small step size in η is used there to accurately approximate the derivatives numerically. On the other hand, far from the plate small changes in the dependent variables are expected. Therefore, a larger step size in η is used there. The initial step size close to the wall $\Delta\eta_1$ used was equal to 0.001. A constant small step size in τ is used (specifically $\Delta\tau = 0.001$) throughout the numerical computations. A representative set of graphical results will be presented and discussed below to illustrate the effects of the behavior coefficient n and the particle loading κ on the solutions.

Figures 1 and 2 show the development of the displacement thicknesses for both the fluid and particulate phase, respectively with time for various behavior coefficient values. The dotted lines in these and subsequent figures correspond to the steady-state solutions reached at large values of τ. It can be seen from these figures that particulate suspensions in dilatant fluids ($n > 1$) approach steady-state conditions faster and have lower displacement thicknesses than those of pseudo-plastic

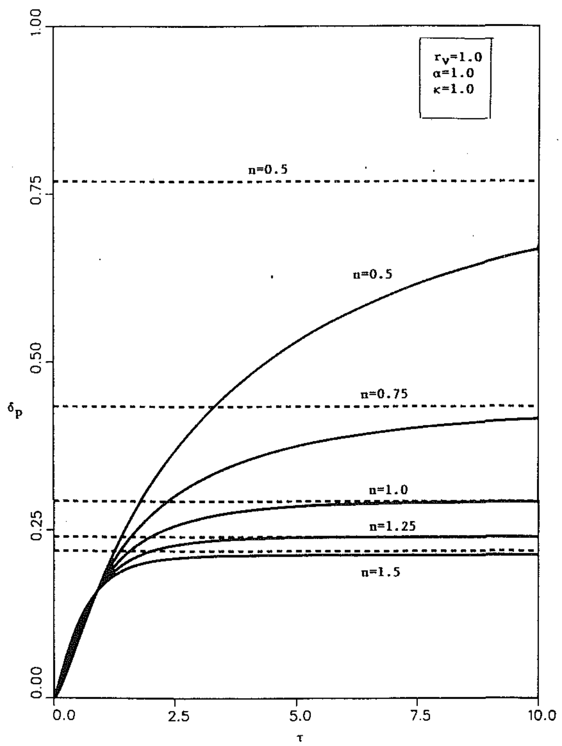

Fig. 2 Particle-phase displacement thickness profiles

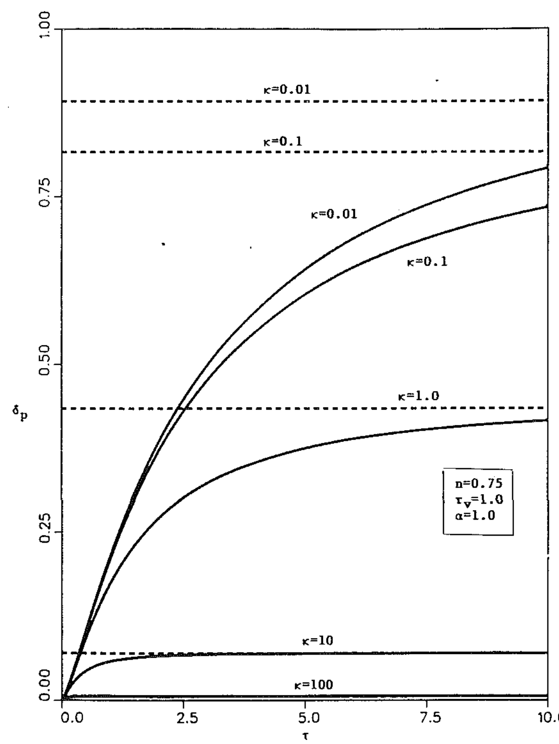

Fig. 4 Particle-phase displacement thickness profiles

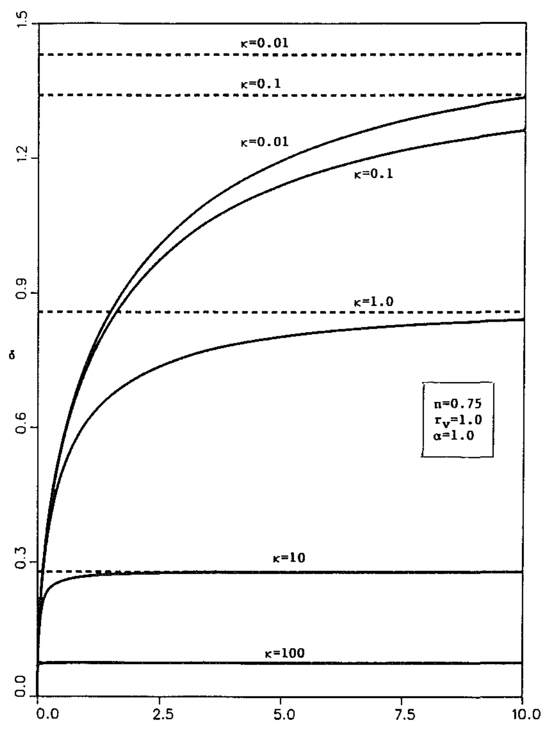

Fig. 3 Fluid-phase displacement thickness profiles

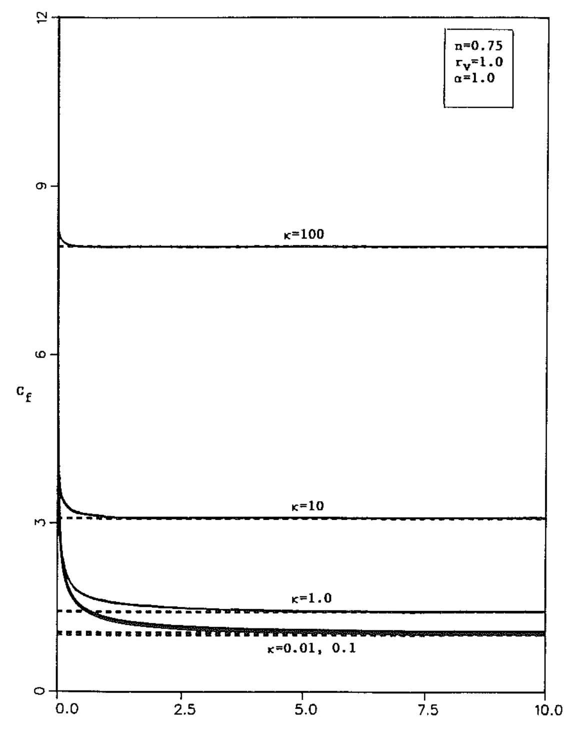

Fig. 5 Fluid-phase skin friction profiles

particulate suspensions. It should be mentioned that while increases in n have a significant effect on δ and δ_p, they appear to have little effect on C_f (figure not shown for brevity).

Figures 3 through 5 illustrate the behavior of δ, δ_p, and C_f versus time for $n=0.75$ and various values of κ, respectively. Increases in the particle loading κ have the tendency to confine viscous effects to an increasingly small region close to the plate surface. This, in turn, causes the slope of the fluid-phase velocity profile at the wall to increase. This is reflected in the decreases in both δ and δ_p and the increases in C_f as κ increases. In Fig. 5 C_f is very large for $\tau << 1$. This is associated with the singularity at $\tau=0$ and is not shown due to the scale of the figure. It should be mentioned that the exact solutions for the dilute limit presented earlier were used as a check on the numerical method and were found to be in excellent agreement with the numerical results.

Conclusions

The transient behavior of a power-law dusty fluid flow past an infinite porous flat plate is solved numerically using an implicit finite-difference scheme. Closed-form solutions for the velocity profiles associated with the dilute steady-state limit are reported. A representative set of graphical results (chosen from many) is presented and discussed. It is hoped that the present work be used as means for understanding more complex problems involving non-Newtonian power-law particulate suspensions.

References

Blottner, F. G., 1970, "Finite Difference Methods of Solutions of the Boundary-Layer Equations," *AIAA Journal*, Vol. 8, pp. 193-205.

Chamkha, A. J., and Peddieson, J., 1989, "Unsteady Dusty-Gas Flow with Suction," presented at the 27th Annual meeting of the Society of Engineering Science.

Hinze, J. O., 1963, "Momentum and Mechanical-Energy Balance Equations for a Flowing Homogeneous Suspension with Slip Between the Two Phases," *Applied Scientific Research*, Vol. A11, pp. 33-46.

Kapur, J. N., 1963, "Flows of Power-Law Fluids Past a Flat Plate with Uniform Suction and Between Two Parallel Plates with Uniform Suction and Injection," *Journal of Physics Society*, Japan, Vol. 18, pp. 578-582.

Marble, F. E., 1970, "Dynamics of Dusty Gases," *Annual Review of Fluid Mechanics*, Vol. 2, pp. 397-446.

Schlichting, H., 1955, *Boundary Layer Theory*, Pergamon Press, pp. 230-232.

Soo, S. L., 1990, *Multiphase Fluid Dynamics*, Science Press, pp. 303-355.